

Assessing weak hydrogen binding on Ca^+ centers: An accurate many-body study with large basis sets

Wirawan Purwanto,* Henry Krakauer, Yudistira Virgus, and Shiwei Zhang
Department of Physics, College of William and Mary, Williamsburg, Virginia 23187-8795, USA
 (Dated: February 17, 2022)

Weak H_2 physisorption energies present a significant challenge to even the best correlated theoretical many-body methods. We use the phaseless auxiliary-field quantum Monte Carlo (AFQMC) method to accurately predict the binding energy of Ca^+-4H_2 . Attention has recently focused on this model chemistry to test the reliability of electronic structure methods for H_2 binding on dispersed alkaline earth metal centers. A modified Cholesky decomposition is implemented to realize the Hubbard-Stratonovich transformation efficiently with large Gaussian basis sets. We employ the largest correlation-consistent Gaussian type basis sets available, up to cc-pCV5Z for Ca, to accurately extrapolate to the complete basis limit. The calculated potential energy curve exhibits binding with a double-well structure.

PACS numbers: 64.70.K-, 71.15.-m, 61.50.Ks, 71.15.Nc.

I. INTRODUCTION

Clean energy economy has become an appealing worldwide endeavor because of its promise of environmental friendliness and economic security. Developing improved hydrogen fuel storage systems for fuel cell applications and finding new technologies for production of hydrogen from renewable sources are important components in achieving this goal. A major standing challenge is the lack of a method for efficient hydrogen storage and retrieval. In developing technologies for on-board hydrogen storage systems, the U.S. DOE has set a target capacity of 9 wt % by year 2015.¹ Physisorption of hydrogen molecules is one mechanism under consideration for use in hydrogen storage. For operation at ambient temperatures, suitable storage media should have a binding strength of $\sim 0.1 - 0.4$ eV per H_2 .^{2,3} However, our current understanding of physisorption processes is still lacking.² First-principles calculations could potentially play an important role in providing insight into the physics of physisorption and identifying suitable media and mechanisms. Achieving predictive accuracy for such weakly bound systems has been problematic, however, for the usually successful density functional theory (DFT) approach and even for explicitly correlated methods.

Dispersed alkaline-earth metal systems have recently shown some promise as H_2 storage media.⁴⁻¹¹ Attention has focused on a simple model chemistry to test the reliability of electronic structure methods in predicting the binding of H_2 on Ca^+ centers. (This is a simplified model which does not take into account the zero-point motion and entropy effects, which are important in modeling real hydrogen storage.) A common thread from these calculations is the prediction and characterization of a double-well potential energy curve (PEC) in the symmetric dissociation of Ca^+-4H_2 . An outer van der Waals well is found in some of the correlated calculations, but not in the DFT calculations with standard local or semilocal exchange-correlation functionals.⁷⁻¹⁰ An inner well (Kubas complex^{12,13}) is found at shorter distances. Overbinding is found in local and semilocal DFT calculations, while explicitly correlated methods yield conflicting results regarding the magnitude of the binding or whether this inner well is even bound.^{7,8,10} Disagreement between the many-

body calculations can be partly attributed to inadequate basis set convergence. The earliest calculation, using the second-order Møller-Plesset perturbation method (MP2), predicted an inner local minimum that is not bound.⁷ Ohk *et al.*⁸ subsequently used MP2 with larger basis sets with an added correction from coupled cluster with singles and doubles and perturbative triples [CCSD(T)] to find both bound inner and outer wells. As we will show in Sec. III, however, the basis sets in Ref. 8 were still too small for accurate extrapolation to the complete basis set (CBS) limit, due to neglect of (semi)core-valence correlation effects. The most recent many-body calculation used diffusion Monte Carlo (DMC) to find an unbound inner well and a barely bound outer well.¹⁰ The current status of theoretical work is clearly unsatisfactory, and the reasons for this need to be clarified and remedied.

The primary objectives of our work are to produce an accurate first-principle PEC of the Ca^+-4H_2 symmetric dissociation process and to clarify the key factors that control the accuracy for many-body calculations. The phaseless auxiliary-field quantum Monte Carlo (AFQMC) method¹⁴⁻¹⁸ with standardized Gaussian type orbital (GTO) basis,¹⁹ hereafter designated as GTO-AFQMC,^{14,17} is used to compute the PEC and to carefully extrapolate the result to the CBS limit. AFQMC has been applied to study a wide variety of material systems.^{14-18,20-26} Its accuracy has been shown to be similar to the gold-standard CCSD(T) method near equilibrium geometries and better for bond-breaking.^{17,23,25,26} The key features of AFQMC include: (1) low algebraic scaling with the system size [$\mathcal{O}(M^3 - M^4)$, where M is the number of the one-particle basis functions]; (2) ease of implementation on massively parallel supercomputers; (3) its wide applicability as an *ab-initio* method in condensed matter physics and quantum chemistry. In the context of quantum chemistry, GTO-AFQMC uses the *identical* basis and Hamiltonian of other standard methods, such as Hartree-Fock (HF), MP2, CCSD(T), and configuration interaction (CI).

In this paper we implement a significant technical improvement in GTO-AFQMC, which removes a computational bottleneck in the preprocessing and initialization step. This allows us to use very large basis sets to obtain accurate ground state energies at the CBS limit. This is made possible by the imple-

mentation of a modified Cholesky decomposition (mCD)^{27–29} of the two-body interaction term in the Hamiltonian. Our GTO-AFQMC calculation with the aug-cc-pCV5Z basis set (827 GTOs) represents the largest many-body calculation in this system with GTOs to date.

The rest of this paper is organized as follows. The implementation of mCD together with relevant methodological details of AFQMC are presented in Sec. II. Accuracy and timing illustrations of AFQMC/mCD are also given. GTO-AFQMC Ca⁺–4H₂ PEC calculations and extrapolation to the CBS limit are presented in Sec. III. In Sec. IV we discuss possible residual sources of error and compare our results to previously published results. We summarize and conclude in Sec. V.

II. GTO-AFQMC METHODOLOGICAL IMPROVEMENTS AND CALCULATION DETAILS

After a brief AFQMC overview, methodological improvements with GTOs are presented. The improvements remove a preprocessing bottleneck for computer time and memory, allowing the use of large GTO basis sets in AFQMC. This is achieved in an unbiased manner using mCD. Accuracy and timing illustrations are given, and the section concludes with the calculation details which are used in Sec. III.

A. AFQMC ground state projection

We briefly review the key features of the phaseless AFQMC method, which are relevant for the remainder of this section. Detailed descriptions of the method can be found in Refs. 14–18.

AFQMC stochastically evaluates the ground state of a many-body Hamiltonian \hat{H} by means of importance sampled random walks in Slater-determinant space.^{14,30} The stochastically generated determinants are the samples of the ground-state many-body wave function $|\Psi_0\rangle$. Although AFQMC is in principle an exact method, in practice the sign or complex-phase problem arises,^{14,30,31} which must be controlled using some approximate means in order to prevent the exponential growth of the Monte Carlo variance. This is done with the phaseless approximation,¹⁴ which has been demonstrated to yield excellent agreement with both experimental and known exact results in a wide variety of molecules and extended systems.^{14,17,18,20–26} To date we have developed AFQMC methods with two basis sets: (1) planewaves with pseudopotentials, which are suitable for studying periodic systems;^{14,18,20,22,24,32} (2) GTOs, which are widely employed for *ab initio* quantum chemistry.^{17,21–23,25,26} In addition there have been many applications on lattice models (*e.g.*, the Hubbard model) where the phaseless approximation reduces to the constrained path approximation^{30,33} due to the nature of the interaction. These systems typically have correlation energy as a significantly higher fraction of their total energy than in most molecules and solids. The high accuracy that has been achieved in these systems for both energy and correlation functions is thus encouraging for the prospect of AFQMC

in real materials.

The electronic Hamiltonian $\hat{H} = \hat{K} + \hat{V}$ contains one-body $\hat{K} = \sum_{ij} K_{ij} c_i^\dagger c_j$ kinetic energy and external potential terms plus two-body electron-electron interaction terms,

$$\hat{V} = \frac{1}{2} \sum_{ijkl} V_{ijkl} c_i^\dagger c_j^\dagger c_k c_l, \quad (1)$$

expressed here in a second quantized form. The fermionic creation operators c_i^\dagger are defined on a finite set of M orthonormal one-particle basis functions $\{\chi_i(\mathbf{r})\}$.

The AFQMC method projects the ground state wave function $|\Psi_0\rangle$ from a trial wave function $|\Psi_T\rangle$,

$$e^{-\tau\hat{H}} e^{-\tau\hat{H}} \dots e^{-\tau\hat{H}} |\Psi_T\rangle \rightarrow |\Psi_0\rangle, \quad (2)$$

using a short-time Trotter-Suzuki decomposition

$$e^{-\tau\hat{H}} = e^{-\tau\hat{K}/2} e^{-\tau\hat{V}} e^{-\tau\hat{K}/2} + \mathcal{O}(\tau^3). \quad (3)$$

The input Ψ_T can be either a single Slater determinant or a multi-determinant wave function; the AFQMC projection yields a stochastic multi-determinant representation of Ψ_0 .

The one-body projector is straightforward to implement in AFQMC: $e^{-\tau\hat{K}/2}$ acting on a Slater determinant yields another Slater determinant. To evaluate the two-body projector $e^{-\tau\hat{V}}$, we first decompose \hat{V} into a sum of squares of one-body operators,³⁴

$$\hat{V} = -\frac{1}{2} \sum_{\gamma} \hat{v}_{\gamma}^2 + (\text{one-body term}), \quad (4)$$

where the minus sign is just a notational convention, and additional one-body terms can arise from reordering the creation and destruction operators. We employ the Hubbard-Stratonovich (HS) transformation^{35,36} to rewrite the two-body projector as a multi-dimensional integral,

$$e^{(1/2)\tau \sum_{\gamma} \hat{v}_{\gamma}^2} \underset{\tau \rightarrow 0}{=} \prod_{\gamma} \int_{-\infty}^{\infty} \frac{d\sigma_{\gamma}}{\sqrt{2\pi}} e^{-\sigma_{\gamma}^2/2} e^{\sqrt{\tau} \sigma_{\gamma} \hat{v}_{\gamma}}. \quad (5)$$

This integral over $\{\sigma_{\gamma}\}$ is evaluated stochastically in AFQMC. Both Eqs. (3) and (5) are exact in the limit $\tau \rightarrow 0$. We therefore have an exact reformulation of the original ground-state projector in terms of one-body projection operators $\{\hat{v}_{\gamma}\}$ coupled with external auxiliary fields $\{\sigma_{\gamma}\}$ which, after integration, recovers the original two-body interactions.³⁴

B. Modified Cholesky decomposition

1. A potential computational bottleneck

The HS decomposition [Eq. (4)] of the two-body interaction term is a preprocessing step, which is done only once at the beginning of the calculation. The decomposition is not unique,

and this flexibility can be exploited to obtain better performance and/or accuracy of the AFQMC calculation.³⁴ The two-body interaction matrix elements V_{ijkl} in Eq. (1) are given by electron-electron Coulomb repulsion integrals (ERIs) in electronic structure calculations:

$$V_{ijkl} = \int d\mathbf{r}_1 d\mathbf{r}_2 \chi_i^*(\mathbf{r}_1) \chi_j^*(\mathbf{r}_2) \frac{e^2}{|\mathbf{r}_1 - \mathbf{r}_2|} \chi_l(\mathbf{r}_1) \chi_k(\mathbf{r}_2). \quad (6)$$

In our earlier implementation of GTO-AFQMC,¹⁷ we used the straightforward approach of diagonalizing the $M^2 \times M^2$ symmetric ERI supermatrix $V_{\mu(i,l),\nu(j,k)}$, where $\mu \equiv (i, l)$ and $\nu \equiv (j, k)$ are compound indices. (The dimension M^2 is reduced by a factor of two with GTOs as they are real-valued.) With the eigenvalues λ_γ and eigenvectors $X_{\mu(i,l)}^\gamma$ of the real, symmetric $V_{\mu\nu}$ supermatrix, the HS one-body operators can be written as

$$\hat{v}_\gamma = \sqrt{-\lambda_\gamma} \sum_{i,l} X_{\mu(i,l)}^\gamma c_i^\dagger c_l. \quad (7)$$

In practice, only $\mathcal{O}(M)$ of the eigenvalues are found to have magnitudes greater than $\sim 10^{-8} E_h$, so the remainder can be discarded. The direct diagonalization leads to an $\mathcal{O}(M^6)$ scaling of computer time and $\mathcal{O}(M^4)$ storage. While exact for any Hermitian two-body interaction, this approach clearly scales poorly with system size.

The HS decomposition described above is a bottleneck for treating large systems. For special choices of the basis, such as planewaves, or for model systems, such as the on-site Hubbard model, the two-body interaction is easily written into the bilinear HS form of Eq. (4), with $\mathcal{O}(M)$ terms. This and the diagonalization results above suggest that the information content in the two-body term is only $\mathcal{O}(M)$ and that more efficient HS strategies could be devised for general basis sets in electronic structure calculations.

The underlying problem here is the sheer size of the two-body supermatrix, which plagues all *ab initio* quantum chemistry methods. A number of approaches have been devised to reduce the computer time and number of integrals that need to be stored. These include density fitting or other auxiliary basis methods,³⁷⁻⁴¹ resolution of Coulomb operator,^{42,43} and mCD.²⁷⁻²⁹

We have chosen to implement the mCD to carry out the HS decomposition in AFQMC. The method, similar to planewave approaches, has a single threshold parameter δ which determines the maximum error in the Cholesky-expanded ERIs. For symmetric, positive semidefinite $V_{\mu\nu}$ supermatrices, this error can be reduced to zero, within machine precision, for sufficiently small δ . In practice, our calculations use δ in the range 10^{-6} to $10^{-4} E_h$, depending the target statistical accuracy in the AFQMC calculation, resulting in $N_{\text{CD}} \lesssim 7.5M$ Cholesky vectors. The algorithm and its performance are discussed next.

2. Implementation of Cholesky decomposition in AFQMC

The symmetric, positive semidefinite ERI supermatrix $V_{\mu\nu}$ is decomposed using a recursive mCD algorithm.^{28,29} Given J Cholesky vectors L_μ^j ($j = 1 \dots J$), $V_{\mu\nu}$ can be expressed as

$$\begin{aligned} V_{\mu\nu} &= \sum_{j=1}^J L_\mu^j L_\nu^j + \Delta_{\mu\nu}^{(J)} \\ &\equiv V_{\mu\nu}^{(J)} + \Delta_{\mu\nu}^{(J)}, \end{aligned} \quad (8)$$

where $\Delta_{\mu\nu}^{(J)}$ is the residual error at the J -th iteration. The $(J+1)$ -th Cholesky vector is obtained from

$$L_\mu^{J+1} = \frac{\Delta_{\mu[\nu]_J}^{(J)}}{\sqrt{\Delta_{[\nu]_J[\nu]_J}^{(J)}}}, \quad (9)$$

where $[\nu]_J$ indicates the index of the largest diagonal element, $\Delta_{[\nu]_J[\nu]_J}^{(J)}$, of the residual error matrix in the J -th iteration. A key point is that only a single column $\Delta_{\mu[\nu]_J}^{(J)}$ need to be computed and stored at any iteration. This iteration is repeated until $\Delta_{[\nu]_J[\nu]_J}^{(J)}$ is less than δ . This procedure guarantees that all matrix elements of the residual matrix are less than δ :

$$\left| V_{\mu\nu} - V_{\mu\nu}^{(N_{\text{CD}})} \right| = \left| \Delta_{\mu\nu}^{(N_{\text{CD}})} \right| \leq \delta \quad (10)$$

where the number of Cholesky vectors corresponding to this δ is denoted by N_{CD} . Damped prescreening²⁹ is applied in each iteration step to stabilize the mCD factorization.

Using the N_{CD} Cholesky vectors, the decomposition in Eq. (4) becomes

$$\begin{aligned} \hat{V} &= \frac{1}{2} \sum_{\gamma=1}^{N_{\text{CD}}} \left(\sum_{il} L_{\mu(i,l)}^\gamma c_i^\dagger c_l \right) \left(\sum_{jk} L_{\nu(j,k)}^\gamma c_j^\dagger c_k \right) \\ &\quad - \frac{1}{2} \sum_{\gamma=1}^{N_{\text{CD}}} \sum_{ijk} L_{\mu(i,j)}^\gamma L_{\nu(j,k)}^\gamma c_i^\dagger c_k \\ &\quad + \mathcal{O}(\delta), \end{aligned} \quad (11)$$

where the extra one-body operator is also explicitly expressed in terms of the Cholesky vectors. The Cholesky vectors translate directly to the matrix elements of \hat{v}_γ in Eq. (4):

$$\hat{v}_\gamma = \sqrt{-1} \sum_{il} L_{\mu(i,l)}^\gamma c_i^\dagger c_l, \quad (12)$$

and the number of auxiliary fields is just given by N_{CD} .

In this work the Cholesky vectors were generated “on the fly” within NWChem⁴⁴ or MPQC.⁴⁵ In GTO-AFQMC, the second-quantized expression for the Hamiltonian must be expressed with respect to orthogonalized GTOs.¹⁷ The mCD procedure [Eq. (8)] is carried out in the original GTO basis, and the resulting Cholesky vectors are then transformed to the orthogonalized basis.

In order to produce high-quality Cholesky vectors which satisfy the accuracy condition Eq. (10), it is imperative that the original ERIs used in the mCD recursive procedure be calculated to very high accuracy and precision. The $V_{\mu\nu}$ supermatrix will not be strictly positive semidefinite (within machine precision) if there are errors in the calculated ERIs. In a test case with $M = 180$, we observe from direct diagonalization of $V_{\mu\nu}$ that there are some negative eigenvalues of $\mathcal{O}(-10^{-8})$. In this case, the resulting Cholesky vectors would not properly reconstitute all the ERIs to within δ accuracy when δ is driven below 10^{-8} . In another test with $M \sim 550$, errors in the calculated ERIs smaller than $10^{-8} E_h$ lead to violation of Eq. (10) with δ set to $\mathcal{O}(10^{-6})$.

3. GTO-AFQMC/mCD accuracy and timing illustrations

Table I compares the accuracy of GTO-AFQMC calculations using mCD with that using direct diagonalization (DD) of the $V_{\mu\nu}$ supermatrix. For each δ shown, we confirmed that all $V_{\mu\nu}$ matrix elements are reproduced with error less than δ . Within statistical uncertainty, the QMC energies are equivalent whether we use DD or mCD with δ ranging from 10^{-8} through $10^{-3} E_h$. For this system, the truncation bias from mCD exceeds the targeted statistical error of $2 \times 10^{-4} E_h$ when $\delta \gtrsim 3 \times 10^{-3} E_h$. Figure 1 plots the error

TABLE I. GTO-AFQMC total energies for several values of the mCD threshold parameter δ for Ca^+-4H_2 ($Z = 2.3 \text{ \AA}$ and $d_{\text{H-H}} = 0.7682 \text{ \AA}$; see text), using the cc-pVTZ basis ($M = 155$). A fixed Trotter time step $\tau = 0.01 E_h^{-1}$ was used for all the calculations. The total energy E_{DD} , obtained from direct diagonalization of $V_{\mu\nu}$, is presented for comparison; the eigenvalue cutoff is also shown. N_γ is the corresponding number of auxiliary-fields. A full rank, symmetric, positive definite $V_{\mu\nu}$ matrix would have required $155^2 = 24025$ Cholesky vectors. All energies are in E_h .

Direct diagonalization		
$V_{\mu\nu}$ eigenvalue cutoff	E_{DD}	N_γ
$\lambda_\gamma > 2 \times 10^{-8}$	-681.42990(20)	2280
Modified CD		
Cholesky δ	E_{mCD}	N_{CD}
10^{-8}	-681.43007(15)	1727
10^{-6}	-681.43003(17)	1120
10^{-5}	-681.42988(20)	850
10^{-4}	-681.42977(18)	643
10^{-3}	-681.42932(19)	511
2×10^{-3}	-681.42991(19)	468
3×10^{-3}	-681.43102(18)	436
3.5×10^{-3}	-681.42958(19)	425
4×10^{-3}	-681.39679(19)	403
5×10^{-3}	-681.39609(17)	379

$E_{\text{mCD}}(\delta) - E_{\text{DD}}$ from Table I. For comparison, the corresponding error in the UHF variational energy, computed using the same set of Cholesky vectors, is also shown and is seen to correlate very well with the AFQMC energies.

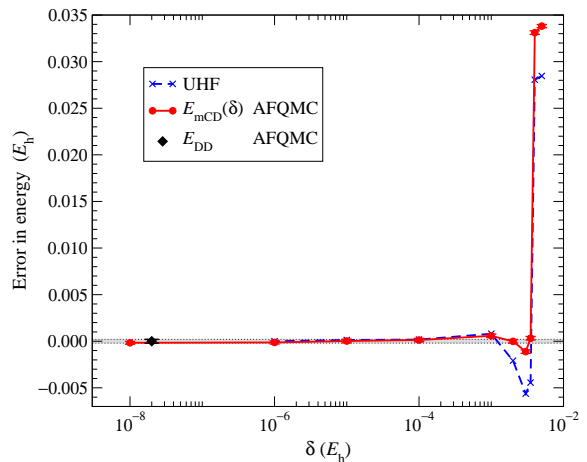


FIG. 1. (Color online) AFQMC total energy error, $E_{\text{mCD}}(\delta) - E_{\text{DD}}$, as a function of the mCD threshold parameter δ , where E_{DD} is the energy obtained from direct diagonalization of the Coulomb matrix (energies are given in Table I). The width of the gray line indicates the statistical uncertainty of E_{DD} . The corresponding error (with respect to the UHF energy) of the trial wave function variational energy is also shown.

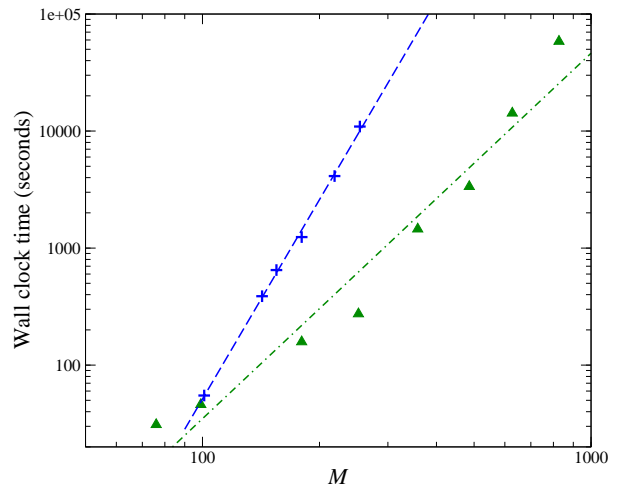


FIG. 2. (Color online) Log-log plots of wall clock times (seconds) vs. basis size M , comparing DD (+) and mCD (\blacktriangle) of the ERI supermatrix $V_{\mu\nu}$. The DD is carried out with 8-thread OpenMP (see text). The mCD timing is obtained from a locally modified MPQC⁴⁵ program, for fixed $\delta = 10^{-6}$. No multithreading is used in the mCD calculations. The dashed (dash-dot) lines are linear regressions. The DD slope $\sim M^{5.7}$ is consistent with the expected M^6 scaling, while mCD scales as $\sim M^{3.1}$.

Figure 2 illustrates the relative timing of DD vs. mCD procedures. Computations were carried out on 64-bit AMD Opteron multi-core processors with speeds ranging from 2.2 GHz up to 3 GHz.⁴⁶ As expected DD times scale as M^6 . The recursive mCD algorithm with prescreening scales only as $\sim M^3$. For the largest ($M = 827$) basis reported in this paper, mCD required less than six hours on a single core, while DD would have taken more than 92 days and nearly 1 TB of memory on the same computer.

Our current mCD implementation still has much room for improvement for application to larger systems. The mCD for the preprocessing HS decomposition has not been parallelized. The sparsity of the Cholesky vectors has also not been exploited for the actual GTO-AFQMC calculations. The decomposition of the necessary $V_{\mu\nu}$ matrix elements scales as $\mathcal{O}(M^3)$ in computer time and the memory required to store the Cholesky vectors also currently scales as $\mathcal{O}(M^3)$. Fully exploiting the sparse structure of the Cholesky vectors would further reduce the memory requirement to $\mathcal{O}(M^2)$ asymptotically for very large molecules.²⁸

C. $\text{Ca}^+ - 4\text{H}_2$ calculation details

As a model of the Ca^+ binding site in a hydrogen storage system, the PEC for symmetric dissociation of $\text{Ca}^+ - 4\text{H}_2$ was calculated as a function of the $\text{Ca}^+ - \text{H}_2$ lateral distance Z (see Fig. 3). For each value of Z , the H-H distance $d_{\text{H-H}}$ is optimized using MP2 with the cc-pCVTZ basis. The UHF wave function is used as the trial wave function Ψ_{T} . GTO-AFQMC calculations were carried out using the correlation-consistent core-valence (cc-pCV x Z) basis set family for $\text{Ca}^{47,48}$ and cc-pV x Z for the H atoms. (This joint basis is subsequently designated as “cc-pCV x Z”.) For some selected geometries, calculations were also carried out using a second basis set family denoted “aug-cc-pCV x Z”, which comprises the cc-pCV x Z functions for Ca and the diffuse aug-cc-pV x Z functions for the H atoms.

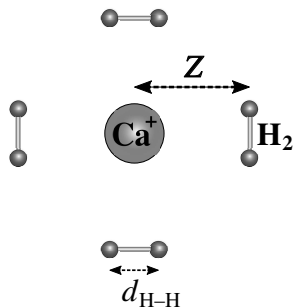


FIG. 3. An illustration of the $\text{Ca}^+ - 4\text{H}_2$ model chemistry, containing one Ca^+ surrounded by four hydrogen molecules in a D_{4h} symmetric configuration.

Extensive basis-set extrapolation tests were carried out to eliminate the errors from the use of finite GTO basis sets. Such tests have not been systematically reported in previous studies of the system. The best CBS extrapolation procedure separately treats the HF and correlation energies,

$$E_{\text{HF}}(\infty) \approx E_{\text{HF}}(x) - B e^{-\alpha x}, \quad (13)$$

$$E_{\text{corr}}(\infty) \approx E_{\text{corr}}(x) - \frac{C}{x^3}, \quad (14)$$

since correlation energy convergence is much slower than HF.⁴⁹⁻⁵² Here x is the correlation consistent basis cardinal number. The HF CBS extrapolation requires calculations with

a minimum of three basis sets, while the correlation energy CBS extrapolation requires at least two.

We examined errors from the Trotter time step τ on basis set extrapolation in GTO-AFQMC. With core-valence basis sets, the absolute energy can vary significantly. At the 5Z level, for example, the error in the absolute energy is as large as $20 mE_{\text{h}}$ for $\tau = 0.01 E_{\text{h}}$. Binding energies, however, are less sensitive, since the $\tau \rightarrow 0$ extrapolation slope for a given basis set was found to be insensitive to the geometry of the system. Binding energies were therefore obtained using a finite time step of $\tau = 0.01 E_{\text{h}}^{-1}$. The validity of this approach was verified by computing energy differences obtained with separate $\tau \rightarrow 0$ extrapolations at representative geometries. For the valence-only basis sets, the total energies change insignificantly under $\tau \rightarrow 0$ extrapolation, and the calculations are always reported at $\tau = 0.01 E_{\text{h}}^{-1}$.

The PEC for the $\text{Ca}^+ - 4\text{H}_2$ binding energy is given by

$$E_{\text{b}}(Z) \equiv E(Z) - E_{\text{frag}}, \quad (15)$$

where E_{frag} is the fragment total energy,

$$E_{\text{frag}} \equiv E_{\text{Ca}^+} + 4E_{\text{H}_2}. \quad (16)$$

In our CBS extrapolation it is convenient to further decompose the binding energy into its HF and correlation contributions,

$$E_{\text{b}}(Z) = E_{\text{b}}^{\text{HF}}(Z) + E_{\text{b}}^{\text{corr}}(Z), \quad (17)$$

In this work the HF total energies are extrapolated using $x \in \{3, 4, 5\}$ in $E_{\text{b}}^{\text{HF}}(Z)$. The ansatz in Eq. (14) implies that $E_{\text{b}}^{\text{corr}}(Z)$ varies linearly with respect to x^{-3} ,

$$\begin{aligned} E_{\text{b}}^{\text{corr}}(Z, \infty) &\approx E_{\text{b}}^{\text{corr}}(Z, x) - \frac{C'(Z)}{x^3} \\ &\equiv E_{\text{b}}^{\text{corr}}(Z, x) + \Delta E_{\text{b}}^{\text{corr}}(Z, x). \end{aligned} \quad (18)$$

$C'(Z)$ is a Z -dependent CBS coefficient. Ideally we would perform AFQMC calculations at all geometries with two or more basis sets to obtain both $E_{\text{b}}^{\text{corr}}(Z, \infty)$ and $C'(Z)$ directly. Such a calculation would be unnecessarily expensive, especially at the largest cc-pCV5Z basis level ($M = 627$). Instead, AFQMC CBS parameters were obtained at several representative geometries (Z) using both the $x \in \{3, 4\}$ and the $x \in \{3, 4, 5\}$ series. We then adopt the following strategy to parametrize $C'_{\text{AFQMC}}(Z)$ and estimate the final PEC. We compute the AFQMC finite-basis $E_{\text{b}}^{\text{corr}}(Z, x)$ with the cc-pCVTZ basis set ($x = 3$). We also assume that, across all Z values, the ratio of correlation energies recovered by AFQMC and MP2 is approximately constant and given by the parameter ρ . The AFQMC CBS correction term can therefore be approximated by scaling the MP2 CBS correction term,

$$\Delta E_{\text{b}}^{\text{corr}}(Z, x, \text{AFQMC}) \approx \rho \Delta E_{\text{b}}^{\text{corr}}(Z, x, \text{MP2}), \quad (19)$$

or, equivalently,

$$C'_{\text{AFQMC}}(Z) \approx \rho C'_{\text{MP2}}(Z). \quad (20)$$

The MP2 energies were computed using the cc-pCVTZ and cc-pCVQZ basis sets to obtain $C'_{\text{MP2}}(Z)$, which determines ρ and the final CBS estimate for the complete AFQMC PEC. We verified that this MP2-assisted approach accurately reproduced direct AFQMC extrapolations at selected geometries to within statistical errors.

Spectroscopic constants associated with the computed PEC were obtained from Morse fits,

$$E_b(Z) = E_0 + \frac{k}{2a^2} \left[1 - e^{-a(Z-Z_0)} \right]^2, \quad (21)$$

where E_0 is the well depth minimum, Z_0 the location of the well minimum, and k is the one-dimensional harmonic spring constant.

III. RESULTS

In modeling the binding of H_2 molecules onto dispersed calcium centers, the convergence with respect to basis set is very delicate. This is illustrated by the all-electron Ca^+-4H_2 PECs in Fig. 4. The solid lines are Morse fits to GTO-AFQMC and MP2 binding energies calculated with the cc-pCVTZ basis set (see Sec. II C for computational details). The symmetric dissociation PECs are seen to exhibit a double-well structure. AFQMC results using larger (cc-pCVQZ and cc-pCV5Z) basis sets are shown at a few selected Z . The inner and outer wells show dramatically different rates of basis set convergence. The inner well does not exhibit binding at the

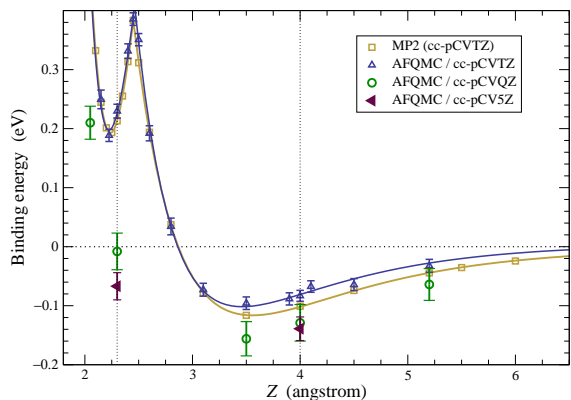


FIG. 4. (Color online) All-electron GTO-AFQMC and MP2 PEC of the Ca^+-4H_2 symmetric dissociation as a function of Z (Ca^+-H_2 separation distance) at the cc-pCVTZ basis level. The solid lines are from separate Morse fits for the inner and outer regions. Also shown at selected Z are GTO-AFQMC results from larger cc-pCVQZ and cc-pCV5Z basis sets. Vertical lines at $Z = 2.3 \text{ \AA}$ and $Z = 4.0 \text{ \AA}$ are a guide to the eye.

cc-pCVTZ level, being $\sim 0.2 \text{ eV}$ higher than the dissociation limit. The outer van der Waals well is bound ($\sim -0.1 \text{ eV}$ at $Z_0 \sim 3.5 \text{ \AA}$). As the basis size is increased, the inner well changes character, becoming $\sim 0 \text{ eV}$ with cc-pCVQZ and then bound by $\sim -0.1 \text{ eV}$ at the cc-pCV5Z level. By contrast, the outer well binding energy is already converged at

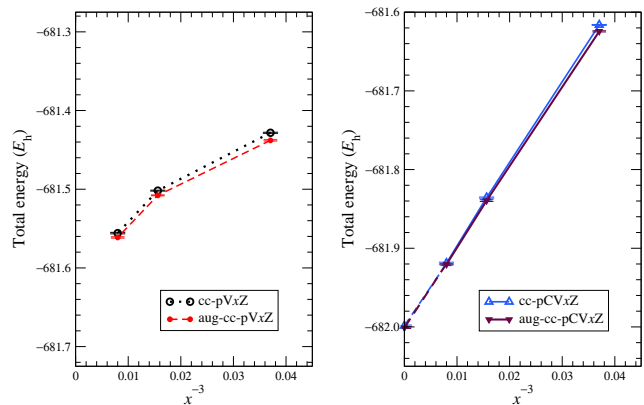


FIG. 5. (Color online) Basis set convergence of GTO-AFQMC Ca^+-4H_2 total energies for $Z = 2.3 \text{ \AA}$ (near the inner well minimum). Energies are plotted as a function of x^{-3} , where $x \in \{3, 4, 5\}$ is the correlation consistent basis cardinal number. Left panel: valence-only cc-pVxZ and aug-cc-pVxZ; right panel: core-valence cc-pCVxZ and aug-cc-pCVxZ.

cc-pCVQZ basis level. Thus careful extrapolation with the basis sets is required in these systems to reach the CBS limit.

We now show that the basis set must well represent the semicore $\text{Ca } 3s$ and $3p$ states for accurate extrapolation. Figure 5 plots the total energies of Ca^+-4H_2 for correlated valence basis sets (cc-pVxZ and aug-cc-pVxZ) and correlated core-valence basis sets (cc-pCVxZ and aug-cc-pCVxZ), as a function of basis cardinal number [$x = (3, 4, 5)$; see Eq. (14)]. The calculations are for $Z = 2.3 \text{ \AA}$, which is near the inner well minimum. With the core-valence basis sets, the energies show linear dependence on x^{-3} , consistent with the ansatz in Eq. (14), while the valence-only series do not. For reference and benchmark purposes, selected GTO-AFQMC total energies are tabulated in Table II.

The importance of proper core-valence treatment is also evident in the binding energies, as shown by Fig. 6, where results for both the inner- and outer-well regions are shown. For comparison, MP2 results are also shown for the inner-well region. The magnitude of core-valence effects is clearly larger in the inner-well region. This is due to the Kubas interaction,^{12,13} involving $\text{Ca}(3d)$ states. Since the spatial extent of the semicore $\text{Ca}(3s,3p)$ is similar to the $\text{Ca}(3d)$ states, core-valence effects are magnified in this region. The CBS extrapolation lowers the inner well minimum by nearly 0.4 eV compared to the cc-pCVTZ basis results. By contrast, the outer well depth is lowered by only $< 0.1 \text{ eV}$. Even at the cc-pCV5Z level the binding energy is still $\sim 0.05 \text{ eV}$ higher than the CBS limit for the inner well, while at the the outer well it has long converged. Figure 6 also shows that the CBS limit is relatively insensitive to the use of diffuse "aug" functions for the H atoms. These results emphasize that it is necessary to use larger core-valence correlation-consistent basis sets in many-body calculations for such weakly bound hydrogen storage systems with binding-site atoms containing semicore states.

In Figs. 5 and 6 we see that, with the cc-pCVxZ basis sets, even the total and binding energies follow the x^{-3} scaling to a very good degree, which is the form for correlation ener-

TABLE II. All electron GTO-AFQMC Ca^+-4H_2 total energies (in E_h) for two geometries and two correlation-consistent core-valence basis sets. “Inner well” corresponds to $Z = 2.3 \text{ \AA}$ and $d_{\text{H-H}} = 0.7682 \text{ \AA}$; “outer well” corresponds to $Z = 4.0 \text{ \AA}$ and $d_{\text{H-H}} = 0.7362 \text{ \AA}$. The total energies of the isolated Ca^+ and H_2 fragments are also shown. The mCD method with $\delta = 10^{-6} E_h$ is used, unless otherwise noted. In all cases, bias from mCD is much smaller than the AFQMC statistical error, which are on the last two digits and are indicated in parentheses. All energies were extrapolated to the $\tau \rightarrow 0$ limit. CBS indicates the complete basis set extrapolated limit.

Basis set	M	inner well $Z = 2.3 \text{ \AA}$	outer well $Z = 4.0 \text{ \AA}$	Ca^+	H_2 $d_{\text{H-H}} = 0.7362 \text{ \AA}$
Basis family: cc-pCV x Z					
$x = 3$	180	-681.61620(61)	-681.62600(71)	-676.93411(28)	-1.17257(11)
$x = 4$	358	-681.83561(74) ^a	-681.84005(76) ^a	-677.13994(45)	-1.17384(18)
$x = 5$	627	-681.9189(12) ^a	-681.92106(77) ^a	-677.21997(52)	-1.17412(15)
CBS	∞	-681.9976(10)	-681.99954(84)	-677.29517(52)	-1.17447(17)
Basis family: aug-cc-pCV x Z					
$x = 3$	252	-681.62437(79)	-681.63180(89)		-1.172826(83)
$x = 4$	486	-681.8395(11)	-681.84151(71)		-1.17397(22)
$x = 5$	827	-681.92056(80) ^b	-681.9213(10) ^b		-1.17434(12)
CBS	∞	-682.00018(94)	-681.99718(99)		-1.17466(14)

^a $\delta = 10^{-5} E_h$

^b $\delta = 10^{-4} E_h$

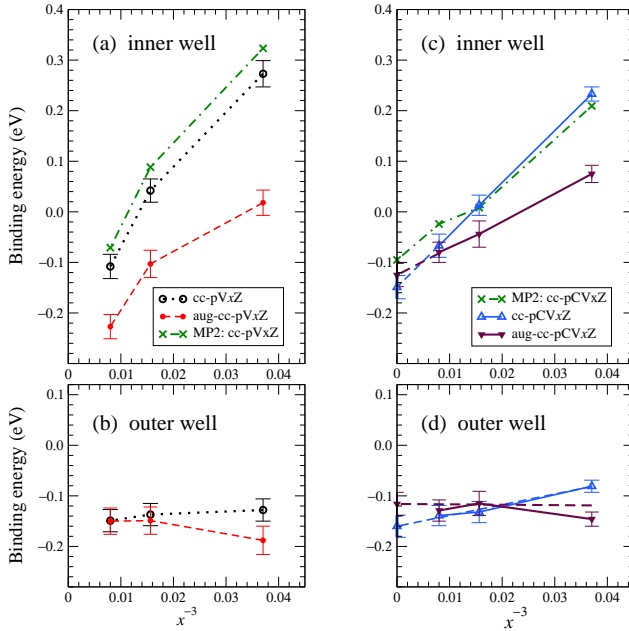


FIG. 6. (Color online) Top panels: The binding energy of Ca^+-4H_2 system near the inner well minimum ($Z = 2.3 \text{ \AA}$, $d_{\text{H-H}} = 0.7682 \text{ \AA}$) plotted against (x^{-3}) , where x is the correlation consistent basis cardinal number. Bottom panels: The binding energy near the outer well minimum ($Z = 4.0 \text{ \AA}$, $d_{\text{H-H}} = 0.7362 \text{ \AA}$).

gies, as shown in Eq. (14). This is so because the HF energy converges rapidly with the basis size, as indicated by Eq. (13). For example, the HF energy changes by roughly $-4 mE_h$ from cc-pCVTZ to the CBS limit across different Z values, in contrast to a change in correlation energy of almost $-400 mE_h$. Similarly, the corresponding HF binding energy changes only by about $-1 mE_h$ (-0.03 eV). Thus, using the procedure described in Sec. II C, the many-body results with

TABLE III. Binding energies E_b after extrapolation to the CBS limit. The two geometries are the same as in Table II (inner well at $Z = 2.3 \text{ \AA}$ and outer well at $Z = 4.0 \text{ \AA}$). The contributions to the AFQMC binding energy [$E_b(Z, \infty)$ on the third row] from HF and correlation are shown separately in the first two rows. Energies are in eV. AFQMC statistical errors are shown in parentheses.

	Inner well	Outer well
$E_b^{\text{HF}}(Z, \infty)$	+0.815	-0.082
$E_b^{\text{corr}}(Z, \infty)$	-0.954(23)	-0.072(22)
$E_b(Z, \infty)$	-0.139(23)	-0.154(22)

core-valence correlation-consistent basis sets can be extrapolated to the CBS limit in a very robust fashion.

Table III shows the extrapolated binding energy results at two representative geometries. HF is qualitatively correct for the outer well, capturing more than half of the well depth. For the inner well, HF is unbound by a very large amount on the scale of interest, by more than 0.8 eV . Thus, consistent with the discussion above on the slow convergence of the Kubas complex, the binding of the inner well is dominated by electron correlation effects, which contribute almost 1 eV to the well depth.

Figure 7 presents the final Ca^+-4H_2 symmetric PEC from GTO-AFQMC calculations, after extrapolation to the CBS limit. The GTO-AFQMC binding energies from the aug-cc-pCV5Z basis set are shown at $Z = 2.3$ and 4.0 \AA to indicate the effect of the extrapolation (recall Fig. 4). The extrapolation of the AFQMC results was done with the procedure described in Sec. II C, assisted by MP2 CBS corrections. As mentioned, this procedure was verified by direct extrapolations of the AFQMC results at two representative geometries using the $x \in \{3, 4, 5\}$ series, as shown in Table III, which gave completely consistent results. In addition, at multiple other geometries, extrapolations of the AFQMC results using

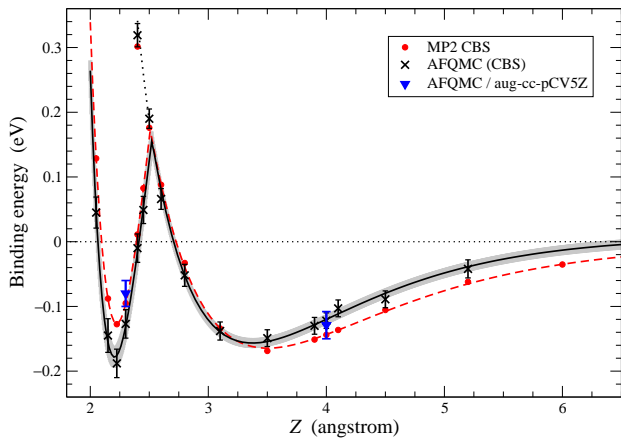


FIG. 7. (Color online) The PEC of the $\text{Ca}^+ - 4\text{H}_2$ symmetric dissociation extrapolated to the CBS limit. The PEC is shown as a function of $\text{Ca}^+ - \text{H}_2$ separation distance, Z . Morse fits to the AFQMC points are shown as solid curves. The gray shading provides an estimate of the PEC uncertainties. Dotted lines shows the continuation of the outer well PEC into the small Z region. Morse fits to the MP2 points are shown as dashed curves. The extrapolation scheme is discussed Sec. II C. For comparison, binding energies computed using very large aug-cc-pCV5Z basis sets are also shown at $Z = 2.3$ and 4.0 Å.

TABLE IV. Spectroscopic constants associated with the AFQMC inner and outer wells depicted in Fig. 7. These parameters were obtained by fitting a Morse curve to the two wells separately. The error bars shown in parentheses below include both the fitting and AFQMC statistical uncertainties.

Quantity	Units	Inner well	Outer well
Well depth minimum E_0	eV	-0.178(16)	-0.1566(71)
Equilibrium distance Z_0	Å	2.205(17)	3.375(41)
Spring constant k	$\text{eV}/\text{Å}^2$	13.0(22)	0.342(37)

the $x \in \{3, 4\}$ series were done as further confirmation, which lead to statistically indistinguishable results at the CBS limit.

The corresponding MP2 results at the CBS limit are also shown. MP2 is seen to represent the double-well structure reasonably well (Figs. 4 and 7). However, there are some significant deviations from AFQMC. The MP2 inner well is more shallow: at the largest basis set (cc-pCV5Z), the MP2 inner-well binding energy is ~ 0.05 eV smaller than AFQMC. The MP2 outer well, by contrast, is deeper and broader than that of AFQMC. This is perhaps not surprising, given the much stronger effect of electron correlation in the inner well region. We comment more on the MP2 results in Sec. IV.

The solid lines with gray shading in Fig. 7 represent Morse fits of the GTO-AFQMC binding energies at the CBS limit, where the width of the shading indicates the uncertainties in the fits. As mentioned, the two regions have separate Morse fits. The fitting uncertainty in the inner well is $\lesssim 0.02$ eV, and $\lesssim 0.01$ eV for the outer well. Spectroscopic constants corresponding to the Morse fitted GTO-AFQMC CBS results are shown in Table IV. The two well minima have comparable well depths within the AFQMC statistical accuracy.

IV. DISCUSSION

In the previous section, the GTO-AFQMC $\text{Ca}^+ - 4\text{H}_2$ PEC was shown to have a double-well structure with weak binding of four H_2 molecules. After extrapolation to the CBS limit, binding energies of $-0.178(16)$ and $-0.1566(71)$ eV were found at the respective minima of the inner and outer wells, essentially the same within statistical errors. The crossover between the two wells occurs at $Z \sim 2.5$ Å. Below we first comment further on possible sources of uncertainty.

A possible source of error in the PEC is the basis set superposition error (BSSE). For a finite basis, when two or more fragments are brought together, the resulting “molecule” enjoys additional degrees of freedom not present in the isolated fragments. This BSSE results in the artificial enhancement of the predicted binding energy. Counterpoise (CP) corrections⁵³ represent an attempt to reduce the BSSE. In the $\text{Ca}^+ - 4\text{H}_2$ system, the effect of the CP correction on HF energies is negligible even at the relatively small cc-pCVTZ basis level. For many-body calculations, we investigated the effect of the CP correction within MP2. The binding energy at the CBS limit was changed by ~ 0.02 eV for the inner well, while the correction in the outer well is negligible. This estimate indicates that the effect of CP correction is within the statistical error of GTO-AFQMC and does not change our conclusions.

A second and related possible source of error is the basis set convergence, as discussed extensively in the previous two sections. This is a system which is particularly demanding in terms of reaching the CBS limit, as we have already shown. The consistency of our various cross-checks suggest that the errors from basis set extrapolation are captured in the indicated uncertainties in Fig. 7 and in Table IV. After we completed this work we were made aware of more recent core-valence basis sets by Iron and co-workers⁵⁴. They have been employed to determine spectroscopic constants for quantum defect calculations in calcium.^{55,56} We have tested these new basis sets, with and without the additional d functions, using MP2 on the $\text{Ca}^+ - 4\text{H}_2$ binding energy at $Z = 2.3$ Å. We found that the binding energy results were consistent with those from the cc-pCV x Z basis sets which we have employed in the present paper. For example, the binding energy at the 5Z level agreed to within 0.003 eV.

A third possible source of error is that our AFQMC method is not exact. The phaseless approximation is made to control the sign/phase problem, and as a result there is a systematic bias. The ground state energies calculated from the method is not guaranteed to be a variational upper bound. As mentioned, for a variety of benchmarks and applications, the systematic bias is shown to be very small, consistently reaching the level of accuracy of CCSD(T). For bond-stretching and bond-breaking, the method is shown to be more accurate than CCSD(T).^{17,23,25,26} For the present systems, internal checks by varying the form of the trial wave function indicate that the results are very robust.

We next compare our results with previous calculations. As discussed in the previous section, MP2 is seen to describe the system quite well. Due to its nonperturbative nature, AFQMC recovers more correlation energy compared to MP2. For ex-

ample, at the CBS limit, the AFQMC Ca^+-4H_2 total energies are $\sim 60 mE_h$ lower at all geometries. Cancellation of errors greatly reduces the discrepancies in the corresponding binding energies. The high symmetry and absence of near-degeneracy in the Ca^+-4H_2 system also makes it easier for MP2 to perform well. The fourfold symmetric Ca^+-4H_2 system is in a half-filled, closed-shell configuration. Open-shell configurations and near degeneracies in other cases would be more challenging.

The CCSD(T)/CBS results of Ohk and co-workers⁸ also predict binding for the both the inner and outer wells. However, Ohk *et al.* used valence-only correlation consistent basis sets, and only up to cc-pVQZ to find the CBS limit. As shown in the previous section, extrapolations with valence-only basis sets is problematic. Moreover, their crossover position is at $Z \sim 2.3 \text{ \AA}$, while our AFQMC and MP2 crossovers are at $Z \sim 2.5 \text{ \AA}$.

In comparing with the DMC results of Bajdich *et al.*,¹⁰ we note that in general DMC is a highly accurate many-body method. Their calculation predicts an inner well that is not bound ($E_0 \sim 0.06 \text{ eV}$) and an outer well that is weakly bound ($E_0 \sim -0.07 \text{ eV}$). Their crossover position is more consistent with our PEC than with the results of Ohk *et al.*⁸ They used $Z = 4.6 \text{ \AA}$ as representative of the unbound fragments. Our result suggests that at $Z = 4.6 \text{ \AA}$ the Ca^+-4H_2 is still weakly bound with $E_b \sim -0.08 \text{ eV}$. Correcting the DMC PEC by this amount increases the DMC outer well binding strength to agree with AFQMC. The DMC inner well remains essentially unbound. The DMC calculations fixed $d_{\text{H-H}} = 0.77 \text{ \AA}$, but our test calculations with AFQMC varying $d_{\text{H-H}}$ show that this only has a small effect on the binding energy, $< 0.01 \text{ eV}$. Thus, the most likely cause for the discrepancy on the inner well would appear to be the fixed-node error in DMC. The use of only triple-zeta quality basis sets in the trial wave functions of the DMC calculations may have contributed to increase this error.

V. SUMMARY

The phaseless auxiliary-field quantum Monte Carlo method was used to accurately predict the binding energy of Ca^+-4H_2 , a model chemistry that has recently been used to test the reliability of electronic structure methods for

H_2 binding on dispersed alkaline earth centers. A modified Cholesky decomposition is implemented to realize the Hubbard-Stratonovich transformation efficiently in AFQMC with large basis sets, which removes a memory and computational bottleneck. We employ the largest correlation consistent Gaussian-type basis sets available, up to cc-pCV5Z for Ca, to accurately extrapolate to the complete basis limit. The resulting potential energy curve exhibits binding with a double-well structure, with nearly equal binding energy minima of $\sim -0.18 \text{ eV}$. We showed that an accurate description of the inner well Kubas complex requires the use of the correlation-consistent core-valence basis set series cc-pCV x Z. While the model's binding energy of $\sim -0.04 \text{ eV/H}_2$ falls short, in itself, of the targeted optimum design value by more than a factor of three, the results are encouraging for further study of larger, more realistic models as potential candidates for hydrogen storage media.

The results in this paper demonstrate that the phaseless AFQMC method can accurately treat the weakly bound systems of interest for hydrogen storage. This is consistent with earlier results on a variety of materials systems. As GTO-AFQMC continues to improve, it can be expected to treat larger, more realistic, nanoscale size systems, with the largest available GTO basis sets. We hope that the latest results will encourage the integration of the GTO-AFQMC method with quantum chemistry approaches, as a component of the community's efforts for improving energy technologies.

ACKNOWLEDGMENTS

The work was supported in part by grants from DOE (DE-SC0001303 and DE-FG05-08OR23340), ONR (N00014-08-1-1235), and NSF (DMR-1006217). This research used resources of the Oak Ridge Leadership Computing Facility, located in the National Center for Computational Sciences at Oak Ridge National Laboratory, which is supported by the Office of Science of the DOE under Contract DE-AC05-00OR22725. We also acknowledge the computing support from the Center for Piezoelectrics by Design. We are grateful to Garnet Chan, Fred Manby, and Todd Martinez for helpful conversations, and to Eric Walter for many useful discussions throughout the course of this work. W.P. would like to thank Jeff Hammond for useful discussions and suggestions.

* wirawan0@gmail.com

¹ U.S. Department of Energy, "Fuel cell technology program: Multi-year research, development and demonstration plan: Planned program activities for 2005-2015," see <http://www1.eere.energy.gov/hydrogenandfuelcells/mypp> (Apr. 2009).

² U.S. Department of Energy, "DOE hydrogen program: 2010 annual progress report," see http://www.hydrogen.energy.gov/annual_progress10.html, in particular Sec. IV.C.1, "Hydrogen Sorption Center of Excellence" (Feb. 2011).

³ S. K. Bhatia and A. L. Myers, *Langmuir* **22**, 1688 (Feb. 2006).

⁴ Y. Y. Sun, K. Lee, Y.-H. Kim, and S. B. Zhang, *Appl. Phys. Lett.* **95**, 033109 (2009).

⁵ Y.-H. Kim, Y. Y. Sun, and S. B. Zhang, *Phys. Rev. B* **79**, 115424 (Mar. 2009).

⁶ H. Lee, J. Ihm, M. L. Cohen, and S. G. Louie, *Phys. Rev. B* **80**, 115412 (Sep. 2009).

⁷ J. Cha, S. Lim, C. H. Choi, M.-H. Cha, and N. Park, *Phys. Rev. Lett.* **103**, 216102 (Nov. 2009).

⁸ Y. Ohk, Y.-H. Kim, and Y. Jung, *Phys. Rev. Lett.* **104**, 179601 (Apr. 2010).

- ⁹ Y. Sun, K. Lee, L. Wang, Y.-H. Kim, W. Chen, Z. Chen, and S. Zhang, *Phys. Rev. B* **82**, 0734401 (Aug. 2010).
- ¹⁰ M. Bajdich, F. A. Reboredo, and P. R. C. Kent, *Phys. Rev. B* **82**, 081405 (Aug. 2010).
- ¹¹ P. B. Sorokin, H. Lee, L. Y. Antipina, A. K. Singh, and B. I. Yakobson, *Nano Lett.* **11**, 2660 (2011).
- ¹² G. J. Kubas, *J. Organomet. Chem.* **635**, 37 (2001).
- ¹³ G. J. Kubas, *Chem. Rev.* **107**, 4152 (Oct. 2007).
- ¹⁴ S. Zhang and H. Krakauer, *Phys. Rev. Lett.* **90**, 136401 (Apr. 2003).
- ¹⁵ W. Purwanto and S. Zhang, *Phys. Rev. E* **70**, 056702 (9 Nov. 2004).
- ¹⁶ W. Purwanto and S. Zhang, *Phys. Rev. A* **72**, 053610 (10 Nov. 2005).
- ¹⁷ W. A. Al-Saidi, S. Zhang, and H. Krakauer, *J. Chem. Phys.* **124**, 224101 (9 Jun. 2006).
- ¹⁸ W. Purwanto, H. Krakauer, and S. Zhang, *Phys. Rev. B* **80**, 214116 (23 Dec. 2009).
- ¹⁹ K. L. Schuchardt, B. T. Didier, T. Elsethagen, L. Sun, V. Gurumoorathi, J. Chase, J. Li, and T. L. Windus, *J. Chem. Inf. Model.* **47**, 1045 (2007).
- ²⁰ W. A. Al-Saidi, H. Krakauer, and S. Zhang, *Phys. Rev. B* **73**, 075103 (2 Feb. 2006).
- ²¹ W. A. Al-Saidi, H. Krakauer, and S. Zhang, *J. Chem. Phys.* **125**, 154110 (19 Oct. 2006).
- ²² W. A. Al-Saidi, H. Krakauer, and S. Zhang, *J. Chem. Phys.* **126**, 194105 (21 May 2007).
- ²³ W. A. Al-Saidi, S. Zhang, and H. Krakauer, *J. Chem. Phys.* **127**, 144101 (2007).
- ²⁴ M. Siewattana, W. Purwanto, S. Zhang, H. Krakauer, and E. J. Walter, *Phys. Rev. B* **75**, 245123 (2007).
- ²⁵ W. Purwanto, W. A. Al-Saidi, H. Krakauer, and S. Zhang, *J. Chem. Phys.* **128**, 114309 (19 Mar. 2008).
- ²⁶ W. Purwanto, S. Zhang, and H. Krakauer, *J. Chem. Phys.* **130**, 094107 (6 Mar. 2009).
- ²⁷ N. H. F. Beebe and J. Linderberg, *Int. J. Quant. Chem.* **12**, 683 (1977).
- ²⁸ H. Koch, A. S. de Merás, and T. B. Pedersen, *J. Chem. Phys.* **118**, 9481 (2003).
- ²⁹ F. Aquilante, L. D. Vico, N. Ferré, G. Ghigo, P. Åke Malmqvist, P. Neogrády, T. B. Pedersen, M. Pitoňák, M. Reiher, B. O. Roos, L. Serrano-Andrés, M. Urban, V. Veryazov, and R. Lindh, *J. Comput. Chem.* **31**, 224 (2010).
- ³⁰ S. Zhang, J. Carlson, and J. E. Gubernatis, *Phys. Rev. B* **55**, 7464 (15 Mar. 1997).
- ³¹ E. Y. Loh Jr., J. E. Gubernatis, R. T. Scalettar, S. R. White, D. J. Scalapino, and R. L. Sugar, *Phys. Rev. B* **41**, 9301 (1990).
- ³² S. Zhang, H. Krakauer, W. A. Al-Saidi, and M. Siewattana, *Comput. Phys. Commun.* **169**, 394 (2005).
- ³³ C.-C. Chang and S. Zhang, *Phys. Rev. B* **78**, 165101 (Oct. 2008).
- ³⁴ S. Zhang, in *Theoretical Methods for Strongly Correlated Electrons*, CRM Series in Mathematical Physics, edited by D. Sénéchal, A.-M. Tremblay, and C. Bourbonnais (Springer, New York, 2003) pp. 39–74.
- ³⁵ R. D. Stratonovich, *Dokl. Akad. Nauk. SSSR* **115**, 1907 (15 Jul. 1957).
- ³⁶ J. Hubbard, *Phys. Rev. Lett.* **3**, 77 (15 Jul. 1959).
- ³⁷ J. L. Whitten, *J. Chem. Phys.* **58**, 4496 (1973).
- ³⁸ O. Vahtras, J. Almlöf, and M. W. Feyereisen, *Chem. Phys. Lett.* **213**, 514 (1993).
- ³⁹ F. Weigend, *Phys. Chem. Chem. Phys.* **4**, 4285 (2002).
- ⁴⁰ H.-J. Werner, F. R. Manby, and P. J. Knowles, *J. Chem. Phys.* **118**, 8149 (2003).
- ⁴¹ F. Neese, *J. Comput. Chem.* **24**, 1740 (2003).
- ⁴² S. A. Varganov, A. T. B. Gilbert, E. Deplazes, and P. M. W. Gill, *J. Chem. Phys.* **128**, 201104 (2008).
- ⁴³ T. Limpanuparb and P. M. W. Gill, *Phys. Chem. Chem. Phys.* **11**, 9176 (2009).
- ⁴⁴ M. Valiev, E. Bylaska, N. Govind, K. Kowalski, T. Straatsma, H. van Dam, D. Wang, J. Nieplocha, E. Apra, T. Windus, and W. de Jong, *Comput. Phys. Commun.* **181**, 1477 (2010).
- ⁴⁵ C. L. Janssen, I. B. Nielsen, M. L. Leininger, E. F. Valeev, J. P. Kenny, and E. T. Seidl, *The Massively Parallel Quantum Chemistry Program (MPQC), Version 2.3.1*, Sandia National Laboratories, Livermore, CA (2008), modified by Wirawan Purwanto, the College of William and Mary, Williamsburg, VA, 2010.
- ⁴⁶ The DD procedure uses the dsyev LAPACK routine provided by the Intel Math Kernel Library (MKL). Each DD run utilizes eight cores using OpenMP. The DD timing only covers the wall clock time required to perform the diagonalization of $V_{\mu\nu}$ supermatrix itself. The mCD calculations were done using a locally modified MPQC code, in which the necessary $V_{\mu\nu}$ matrix elements were computed on-the-fly. Our reported mCD timings therefore include the time to compute these matrix elements.
- ⁴⁷ K. A. Peterson and T. H. Dunning, Jr., *J. Chem. Phys.* **117**, 10548 (2002).
- ⁴⁸ J. Koput and K. A. Peterson, *J. Phys. Chem. A* **106**, 9595 (2002).
- ⁴⁹ T. Müller, “Basis sets, accuracy, and calibration in quantum chemistry,” in *Computational Nanoscience: Do It Yourself!*, NIC Series, Vol. 31, edited by J. Grotendorst, S. Blügel, and D. Marx (John von Neumann Institute for Computing, Jülich, 2006) pp. 19–43.
- ⁵⁰ D. Feller, *J. Chem. Phys.* **98**, 7059 (1993).
- ⁵¹ T. Helgaker, W. Klopper, H. Koch, and J. Noga, *J. Chem. Phys.* **106**, 9639 (1997).
- ⁵² A. Halkier, T. Helgaker, P. Jorgensen, W. Klopper, and J. Olsen, *Chem. Phys. Lett.* **302**, 437 (1999).
- ⁵³ F. B. van Duijneveldt, J. G. C. M. van Duijneveldt-van de Rijdt, and J. H. van Lenthe, *Chem. Rev.* **94**, 1873 (1994).
- ⁵⁴ M. A. Iron, M. Oren, and J. M. L. Martin, *Mol. Phys.* **101**, 1345 (2003).
- ⁵⁵ J. J. Kay, S. L. Coy, V. S. Petrović, B. M. Wong, and R. W. Field, *J. Chem. Phys.* **128**, 194301 (2008), ISSN 00219606.
- ⁵⁶ J. J. Kay, S. L. Coy, B. M. Wong, C. Jungen, and R. W. Field, *J. Chem. Phys.* **134**, 114313 (2011), ISSN 00219606.